ISSN: 2472-3703 DOI: 10.6911/WSRJ.202506_11(6).0005

Study on Suspension Parameters Selection of Suspended Equipment under Carbody for High-speed Train Considering Multi-excitation Condition

Meng Xu, Linling Wang, Junjie Chen and Xiaolong He*

School of Mechanical and Electrical Engineering, Chongqing University of Arts and Sciences, Chongqing, 402160, China

* Corresponding author

Abstract

It is confirmed that the suspended equipment under carbody of high speed train are related to the ride comfort of vehicle, vibration severity of equipment. The reason for that is their large mass, able to visibly influence the vibrations of the vehicle. This paper examines the influence of the transformer equipment upon the ride comfort index of vehicle and the vibration severity of equipment considering multi-excitation. These vibration indexes are derived from the numerical simulations developed on a rigid-flexible coupled model using numerical integral method. As a rule, the results prove the influence of the equipment suspension parameters (frequency, position and damping ratio), along with the speed regime, upon the level of ride comfort index of vehicle and equipment vibration severity. Similarly, it is also demonstrated how to select the suspension parameter of equipment considering the dynamic vibration behavior of high speed trains.

Keywords

High speed train; Vehicle-equipment coupling system; Vibration severity; Ride comfort index; Suspension parameters.

1. INTRODUCTION

The vehicle vibration issue is becoming more and more serious due to the continuous improvement of operational speed although high-speed railway has become the most convenient and comfortable mode of transportation for the public. The ride comfort of vehicle and the vibration of under car equipment have been deteriorated with the light weight design and power distribution technique being widely used in vehicle manufacturing. The vehicle equipment system is shown as Fig. 1. Some functional equipment, such as traction transformer, traction converter, and waste collection unit are directly suspended under the vehicle chassis. Among them the traction transformer (as shown in Fig. 2 (a)) is the most typical equipment weighing approximately 4～6 tons and carrying complex excitation [1]. Whether the suspension parameters (as shown in Fig. 2 (b)) of the equipment is reasonable or not has been directly related to the ride comfort of vehicle, fatigue life of the suspension structure and the working vibration environment of the equipment itself.

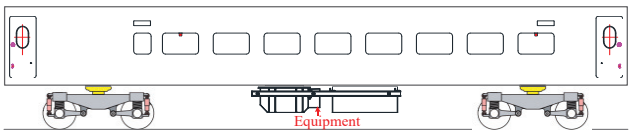


Figure 1. Schematic diagram of vehicle equipment system.

ISSN: 2472-3703 DOI: 10.6911/WSRJ.202506_11(6).0005

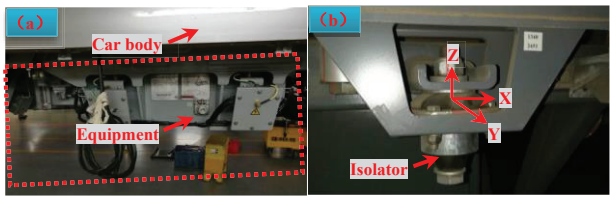


Figure 2. Traction transformer under carbody: (a) Traction transformer, (b) Isolator of transformer

However, there is no corresponding industry standard or methods for how to design suspension parameters of under car equipment of high speed trains. In addition, the complex track excitement and incentives of equipment itself increase the difficulty of suspension parameters design. Hence, a precise design of the suspension parameters of the equipment is imperative.

In recent years, several studies have been conducted on the suspension parameters of equipment. Yao et al. proposed a multi-objective optimization method for bogie suspension parameters of high-speed trains, significantly improving the lateral stability under different wheel-rail contact conditions[2]. Shi et al. conducted an in-depth analysis of the influence of suspension parameters on vehicle modal characteristics, providing a theoretical basis for suspension parameter optimization[3]. Qiu et al. presented an optimization method for the vertical suspension system of high-speed trains based on the particle swarm optimization (PSO) algorithm and verified its effectiveness through simulations[4]. Chen et al. effectively suppressed the hunting motion of high-speed trains and improved their lateral stability by optimizing suspension parameters through a multi-objective approach[5]. Zhu et al. studied the influence of suspension parameters on the vibration characteristics of traction drive components of high-speed trains, providing a reference for the design of traction motor suspension systems[6]. Guo et al. revealed the relationship between the vibration characteristics of suspended equipment on high-speed train car bodies and car body vibrations through field measurements[7]. Dumitriu investigated the influence of suspended equipment on the flexible vibrations and ride comfort of high-speed railway vehicle car bodies using numerical methods[8]. Additionally, Yao et al. explored the robust and adaptive design of suspension parameters for high-speed trains to improve the lateral stability under varying wheel-rail contact conditions[9].

Despite some preliminary advancement in the parameter design of the suspended equipment under carbody, there are a few significant limitations. First, the equipment suspension parameters design do not consider the impact of excitation of the under carbody equipment; Second, the suspension design of under carbody equipment have not considered the effect of parameters on the suspended device vibration behavior which should fulfill the relevant requirements, However, few studies focus on the vibration characteristic of suspended equipment.

This paper puts forward a novel design method for hanging parameters of suspended equipment. Novelties of the proposed method lie in two aspects. One is the way in which the optimal suspension frequency is obtained considering ride comfort index of vehicle and vibration severity of equipment and the other is that suspension parameters of under car equipment were explored with the combination excitation of wheel-rail and transformer self-excitation.

2. MECHANICAL MODEL OF VEHICLE

Fig. 3 shows the coupled vehicle-equipment model [10-11]. The vehicle system comprises a carbody, two bogies, four wheelsets, and suspended equipment. The running speed of the vehicle is *v*, and it is presumed that the wheels are in full contact with the rails. In addition, the

ISSN: 2472-3703 DOI: 10.6911/WSRJ.202506_11(6).0005

carbody is considered as an Euler–Bernoulli beam. The beam parameters are defined in terms of the carbody, such as J_c–inertia moment; L–beam length; $\rho=m_c/L$–beam mass per unit length; where m_c is carbody mass; u–damping coefficient of the carbody; EI–the flexural rigidity, where E is the longitudinal modulus of elasticity, and I is the area moment of inertia of the beam cross-section.

The vehicle suspensions are modeled by means of the Kelvin-Voigt systems. The features of the elastic connections of the secondary are represented by the elastic constant values on vertical direction k_{cz}, longitudinal k_{cx} and the pitch angle stiff

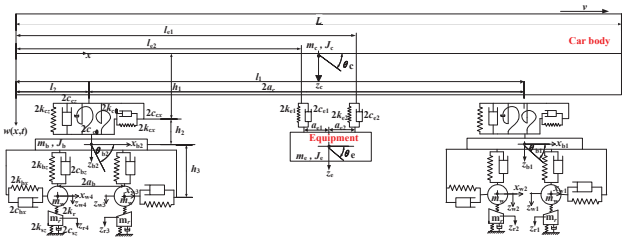


Figure 3. Rail vehicle model.

-ness $k_{c\theta}$, as well as the damping constant values c_{cz}, c_{cx}, and $c_{c\theta}$. For the primary level of suspension, the elastic values are noted with k_{bz}—on vertical direction and k_{bx}—on longitudinal direction, while the damping ones are c_{bz}, c_{bx} respectively.

Carbody rigid vibration modes–bounce z_c and pitch θ_c, and the first carbody vertical bending mode $X_c(x)$. The carbody vertical movement $w(x,t)$ comes from the superposition of the two rigid vibration modes with the first bending mode [12].

$$w(x,t)=z_c(t)+(x-2/L)\theta_c(t)+X_c(x)T_c(t) \tag{1}$$

where $T_c(t)$ is the time coordinate of the first natural bending mode and eigen function of vertical bending is

$$X_c(x)=-\frac{\sin\beta L-\sinh\beta L}{\cos\beta L-\cosh\beta L}(\cos\beta x+\cosh\beta x)+\sin\beta x+\sinh\beta x \tag{2}$$

$$\beta=\sqrt[4]{\omega_c^2\rho_c/(EI)} \tag{3}$$

$$\cos\beta L\cosh\beta L-1=0 \tag{4}$$

where ω_c is the natural frequency of first vertical bending mode. The bogies comprise three degrees of freedom–bounce z_{bi} , pitch θ_{bi}, and longitudinal movement x_{bi}, with i = 1 , 2. Each bogie has the mass m_b, inertia moment J_b and wheelbase $2a_b$.The wheelsets have two degrees of freedom–bounce z_{wj} and longitudinal movement x_{bj}. Each wheelset has the mass m_w. The rail mass under wheelset is m_r, and its bounce is z_{rj} , with j =1,2,3,4.

Equipment vibration modes–bounce z_e and pitch θ_e will be taken into account. The mass of equipment is m_e, and inertia moment is J_e. The distance between suspension position and mass center of equipment are a_{e1}, a_{e2} respectively. The vehicle suspension parameters are listed in Table 1.

ISSN: 2472-3703 DOI: 10.6911/WSRJ.202506_11(6).0005

Table 1. Suspension parameters of vehicle system.

m_c (kg)	27041	J_c(kg·m^2)	1714217
m_b(kg)	2439	J_b(kg·m^2)	1205
m_e(kg)	6400	J_e(kg·m^2)	6364
k_{cz}(MN·m^{-1})	0.61	c_{cz}(kNs·m^{-1})	17.22
m_r(kg)	1713	a_b(m)	1.25
L(m)	25	c_{cx}(kNs·m^{-1})	3
k_{cx}(MN·m^{-1})	0.133	$c_{c\theta}$(kNs·m^{-1})	1
$k_{c\theta}$(kN·m^{-1})	128	c_{bz}(kNs·m^{-1})	3
k_{bz}(MN·m^{-1})	0.9	c_{bx}(kNs·m^{-1})	1
k_{bx}(MN·m^{-1})	0.3	h_1(m)	0.852
k_r(MN·m^{-1})	1500	h_3(m)	0.189
h_2(m)	0.262	l_2(m)	21.401
l_1(m)	3.599	a_{e2m}(m)	1.1
a_{e1}(m)	2.5	c_{sz}(kNs·m^{-1})	20
k_{sz}(MN·m^{-1})	70		

3. EQUATIONS OF VEHICLE SYSTEM MOTION

The vertical motion of vehicle is described by both the equations of rigid mode vibration in carbody and bogie and the equations of the vertical bending mode of carbody. The equations of motion of the car body is written as

$$EI\frac{\partial^4 w(x,t)}{\partial x^4}+\mu I\frac{\partial^5 w(x,t)}{\partial t\partial x^4}+\rho\frac{\partial^2 w(x,t)}{\partial t^2}=\sum_{j=1}^{2}F_{zej}\delta\left(x-l_{ej}\right)+\sum_{i=1}^{2}\left[F_{zci}\delta\left(x-l_i\right)-\left(M_{ci}-h_cF_{xci}\right)\frac{d\delta\left(x-l_i\right)}{dx}\right] \tag{5}$$

where $\delta(x)$ is the Dirac delta function; F_{zej} is the force applied by the equipment on the car body; F_{zci} is the force of the secondary vertical support; M_{ci} is the moment of force applied by the bogies on the car body; F_{xci} is the longitudinal force applied by the bogies on the car body

$$F_{zej}=-2c_{ej}\left[\frac{\partial w\left(l_{ej},t\right)}{\partial t}-\left(\dot{z}_e\pm a_{ej}\dot{\theta}_e\right)\right]-2k_{ej}\left[w\left(l_{ej},t\right)-\left(z_e\pm a_{ej}\theta_e\right)\right] \tag{6}$$

$$F_{zci}=-2c_{cz}\left[\frac{\partial w(l_i,t)}{\partial t}-\dot{z}_{bi}\right]-2k_{cz}\left[w(l_i,t)-z_{bi}\right] \tag{7}$$

$$M_{ci}=-2c_{c\theta}\left[\frac{\partial^2 w(l_i,t)}{\partial x\partial t}-\dot{\theta}_{bi}\right]-2k_{c\theta}\left[\frac{\partial w(l_i,t)}{\partial}-\theta_{bi}\right] \tag{8}$$

ISSN: 2472-3703 DOI: 10.6911/WSRJ.202506_11(6).0005

$$F_{xci} = 2c_{cx}\left[h_1\frac{\partial^2 w(l_i,t)}{\partial x \partial t} + \dot{x}_{bi} + h_2\dot{\theta}_{bi}\right] + 2k_{cx}\left[h_1\frac{\partial w(l_i,t)}{\partial x} + x_{bi} + h_2\theta_{bi}\right] \tag{9}$$

By substituting Eq.(1) into Eq.(5) and integrating along the length of car body, and considering the orthogonality of shape functions and the characteristic of Dirac function, one obtains

$$m_c\ddot{z}_c = \sum_{i=1}^{2} F_{zci} + \sum_{i=1}^{2} F_{zei} \tag{10}$$

$$J_c\ddot{\theta}_c = \sum_{i=1}^{2} F_{zci}(l_i - L/2) + \sum_{i=1}^{2} F_{zei}(l_{ei} - L/2) \tag{11}$$

$$m_m\ddot{T}_2 + c_m\dot{T}_2 + k_mT_2 = \sum_{i=1}^{2} F_{zci}X_2(l_i) + \sum_{i=1}^{2} F_{zei}X_2(l_{ei}) \tag{12}$$

where m_m, c_m, k_m are the stiffness, damping and the modal mass of the carbody respectively. The equations defining the movement of bounce, pitch and longitudinal movement are

$$m_b\ddot{z}_{bi} = \sum_{j=2i-1}^{2i} F_{zbj} - F_{zci}, i = 1,2 \tag{13}$$

$$J_{\mathrm{b}}\ddot{\theta}_{\mathrm{bi}} = \sum_{j=2i-1}^{2i}\left[a_{\mathrm{b}}(-1)^{j+1}F_{zbj} - h_3F_{xbj}\right] - M_{ci} - h_2F_{xci}, i = 1,2 \tag{14}$$

$$m_b\ddot{x}_{bi} = \sum_{j=2i-1}^{2i} F_{xbj} - F_{xci}, i = 1,2 \tag{15}$$

where F_{xbj} are the longitudinal forces derived from the primary suspension of axle j, and F_{zbj} are the vertical forces derived from the primary suspension of axle j. The bounce and pitch motions of suspended equipment are included in the equations

$$m_e\ddot{z}_e = \sum_{i=1}^{2}\left\{-2c_{ej}\left[\frac{\partial w(l_{ej},t)}{\partial t} - (\dot{z}_e \pm a_{ej}\dot{\theta}_e)\right] - 2k_{ej}\left[w(l_{ej},t) - (z_e \pm a_{ej}\theta_e)\right]\right\} \tag{16}$$

$$J_e\ddot{\theta}_e = \left(lei - \frac{L}{2}\right)\sum_{i=1}^{2}\left\{-2c_{ej}\left[\frac{\partial w(l_{ej},t)}{\partial t} - (\dot{z}_e \pm a_{ej}\dot{\theta}_e)\right] - 2k_{ej}\left[w(l_{ej},t) - (z_e \pm a_{ej}\theta_e)\right]\right\} \tag{17}$$

ISSN: 2472-3703 DOI: 10.6911/WSRJ.202506_11(6).0005

The equations of the longitudinal motion of the wheelsets

$$m_{\mathrm{w}}\ddot{x}_{\mathrm{wj}} = -F_{xbj} \tag{18}$$

The equation of the vertical motion of the wheelsets

$$m_w\ddot{z}_{wj} = 2Q_j - F_{zbj} \tag{19}$$

where Q_j is the vertical dynamic contact forces of wheel–rail.

4. ANALYSIS OF MULTI-EXCITATION CONDITION OF VEHICLE SYSTEM

In this work, the multi-excitation of vehicle system consisting of rail-wheel excitement and equipment active excitation are considered. The track irregularity spectra of German railways were used as the wheel-rail excitation. And the traction transformer with excitation is selected as the typical suspended equipment.

4.1. The excitation forces of the track vertical irregularities

The study of the vehicle system vertical vibration involves the hypothesis that the vehicle runs on a track with random defects. In order to evaluate the comfort at vertical vibrations, there will be taken into account the track irregularities as being random and stationary. The track irregularity power spectral density the German railways is looked featured below

$$S(\Omega) = \frac{A\Omega_C^2}{\left(\Omega^2 + \Omega_r^2\right)\left(\Omega^2 + \Omega_C^2\right)} \tag{20}$$

where Ω is the wave number, Ω=0.8246 rad/m, Ω=0.0206 rad/m, and A=4.032·10^{-7} rad·m or A=1.08·10^{-6} rad·m, depending on the track quality.

While noticing that the track defects become an excitation factor for the vehicle travelling at speed v, the spectral density power of the nivelment defects has to be expressed in dependence of the angle frequency $\omega = v \cdot \Omega$, as per the general relation

$$G(\omega) = \frac{S(\omega/v)}{v} \tag{21}$$

The equations (20) and (21) will give

$$G(\omega) = \frac{A\Omega_C^2 v^3}{\left[\omega^2 + \left(v\Omega_C\right)^2\right]\left[\omega^2 + \left(v\Omega_r\right)^2\right]} \tag{22}$$

As we all know, the time-domain analyzing method can make great effectiveness for non-linear system, thus the wheel-rail excitation input described in equation (23) is translated into time domain samples. Here the trigonometric series method was introduced and described below

$$x(d) = \sum_{k=1}^{N} a_k \cos\left(\omega_k d + \phi_k\right) \tag{23}$$

ISSN: 2472-3703 DOI: 10.6911/WSRJ.202506_11(6).0005

where $x(d)$ –Track irregularity sample sequence, k–Sampling point, N–Total sampling points, ak–Amplitude of irregularity, ω_k–Sampling frequency, φ_k–initial phase which is the independent variable from 0 to π.

For given track irregularity power spectral $S_x(\omega)$, the frequency interval is featured

$$\Delta\omega = \frac{\omega_u - \omega_l}{N} \tag{24}$$

Where ω_u and ω_l are the upper and lower cut-frequencies respectively. Also a_k and ω_k can be described as

$$\omega_k = \omega_l + (k - 0.5)\Delta\omega \tag{25}$$

$$a_k = 2\sqrt{S_x(\omega_k)\Delta\omega} \tag{26}$$

With the combination of equations (20)～(26), the vertical irregularity displacement under different velocities are simulated as shown in Fig. 4.

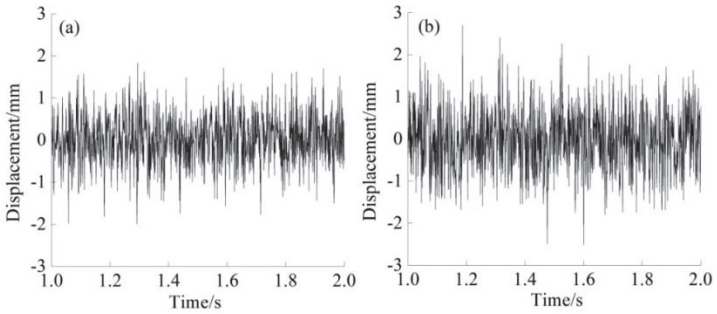


Figure 4. Vertical irregularity displacement: (a) v=200km/h, (b) v=300km/h.

4.2. The excitation forces of the track vertical irregularities

The traction transformer is the equipment which is used to convert 25 kV high voltages into suitable operating voltage for other electrical equipment. It weighs tons and bear intricate excitation sources such as the cooling fans and transforming, and the vibration characteristic of transformer has serious effect on the ride comfort of high speed train.

The equipment (see Fig. 5) comprises transformer body (Fig. 5 (A)) and cooling fans (Fig. 5 (B), Fig. 5 (C)). The incentives of transformer contains three kind of excited source: the excitation generated by the coil winding under the action of electromotive force, the excitation of iron core caused by magnetostrictive effect and the excitation caused by unbalance of rotor of cooling fan.

ISSN: 2472-3703 DOI: 10.6911/WSRJ.202506_11(6).0005

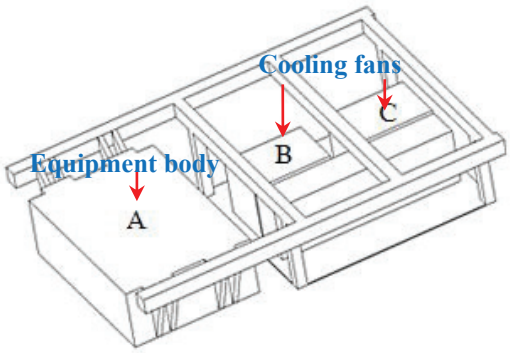


Figure 5. Structure chart of traction transformer.

The excitation of electromotive force can be described as

$$F_r = -\omega_0^2 F_1 e^{-j2\omega_0 t} \sin(\omega_0 t + \theta) - 4\omega^2 F_2 \sin(2\omega t + \varphi) \tag{27}$$

Where F_1 is the excitation amplitude of coil winding vibration; F_2 is the excitation amplitude of forced vibration of coil winding; ω_0 is the natural frequency of coil winding; ω is the frequency of forced vibration; and θ、φ are initial phases.

The excitation force of iron core caused by magnetostrictive effect can be written as

$$F_t = F_{c\max} \sin 2\omega t + \sum_{i=4}^{2n} F_i \sin i\omega t \tag{28}$$

$$F_c = \frac{1}{2}\nabla\left(H^2 \tau \frac{\partial u}{\partial \tau}\right) \tag{29}$$

where $\frac{\partial u}{\partial \tau}$ is the ratio of permeability varies with volume density; H is the magnetic field strength; And τ is the volume density of the medium. The excitation force caused by unbalance of rotor of cooling fan can be indicated

$$F(t) = m_0 \cdot e_0 \cdot \omega_0^2 \cdot \sin \omega_0 t \tag{30}$$

where m_0 is the unbalanced mass of the rotating part; e_0 is the eccentricity, and e_0 is 0.25 in this study; ω_0 is the angular velocity of fan rotor, with ω_0=0.105 n_0, and n_0 is the rotational speed. With the combination of calculation method of excitation force above, the excitation force of the transformer body can be described as

$$F_b = F_1 \sin 2\pi f_1 t + F_2 \sin 2\pi f_2 t + F_3 \sin 2\pi f_3 t \tag{31}$$

The excitation force of cooling fan can be written as

$$F_f = F_4 \sin \omega_1 t + F_5 \sin \omega_2 t \tag{32}$$

The physical parameters in Eq.(31) and Eq.(32) are listed in Table 2.

ISSN: 2472-3703 DOI: 10.6911/WSRJ.202506_11(6).0005

Table 2. Excitation force parameters of transformer.

Excitation frequency of baseband(f_1–Hz)	50
Excitation frequency of second harmonic(f_2–Hz)	100
Excitation frequency of third harmonic(f_3–Hz)	200
Angular frequency of rotational speed 1(ω_1–rad/s)	305.2
Angular frequency of rotational speed 2(ω_2–rad/s)	152.6

The time history curve of excitation force of transformer is shown in figure 6.

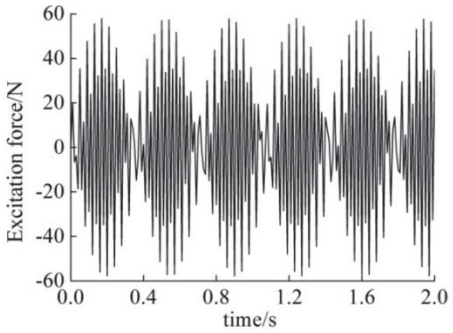


Figure 6. Excitation force of traction transformer.

5. CALCULATION METHOD OF VIBRATION INDEX OF VEHICLE SYSTEM

How to evaluate the vibration level is solved with the combination of ride comfort index and vibration severity of transformer. The ride comfort index is usually used to evaluate the ride comfort of vehicles, and the index of vibration severity is the indicator to estimate the vibration level of suspended equipment.

5.1. The assessment of the ride comfort index

Using the method described in the guidelines of UIC 513R: Guidelines for Evaluating Passenger Comfort in Relation to Vibration in Railway Vehicles to evaluate ride comfort index of passenger [14]. The calculation formula is

$$N = 6\sqrt{\left(a_x^{W_d}\right)^2 + \left(a_y^{W_d}\right)^2 + \left(a_z^{W_b}\right)^2} \tag{33}$$

where N is the ride comfort index; a is the effective value of acceleration; superscripts W_d and W_b are the frequency weighting functions of horizontal and vertical acceleration, respectively; and subscripts x, y, and z are vertical, lateral, and longitudinal direction, respectively. In this research, only the vertical vibration response of vehicle system is calculated and obtained. Hence, Eq. (33) is rewritten as

$$N = 6a_z^{W_b} \tag{34}$$

5.2. Computing method of vibration severity for transformer

Here, the vibration severity of the traction transformer is solved in the frequency domain. For the vibration signal $x(n)$ at point N, the sampling frequency is f_s. Thus, Discrete Fourier transforms (DFT) yields [15]

ISSN: 2472-3703 DOI: 10.6911/WSRJ.202506_11(6).0005

$$X(k)=\sum_{n=0}^{N-1}x(n)e^{-j2nk\pi/N},k=0,1,...,N-1 \tag{35}$$

The single-sided amplitude spectrum is

$$A_k=\frac{2}{N}\left|X(k)\right|,k=0,1,...,N/2-1 \tag{36}$$

Furthermore, the corresponding frequency is

$$f_k=\frac{k\cdot f_s}{N},k=0,1,...,N/2-1 \tag{37}$$

Let $x(n)$ be the vibration acceleration signal in mm/s^2. Then, the vibration severity in the frequency range of $f_a \sim f_b$ is given by

$$V_{rms}=\frac{1}{\sqrt{2}\pi f_s}\sqrt{\sum_{k=k_a}^{k_b}\left(\frac{\left|X(k)\right|}{k}\right)^2} \tag{38}$$

6. NUMERICAL INTEGRATION ALGORITHM FOR VEHICLE EQUIPMENT COUPLED SYSTEM

Here, we used the new and rapid numerical integration method proposed by academician Zhai Wanming to solve the response of the vehicle system [13]. The calculation method is as follows:

The Newmark Hypotheses is made firstly:

$$\begin{cases}\{X\}_{n+1}=\{X\}_n+\{\dot{X}\}_n\Delta t+(1/2-\beta)\{\ddot{X}\}_n\Delta t^2+\beta\{\ddot{X}\}_{n+1}\Delta t^2\\ \{\dot{X}\}_{n+1}=\{\dot{X}\}_n+(1-\gamma)\{\ddot{X}\}_n\Delta t+\gamma\{\ddot{X}\}_{n+1}\Delta t\end{cases} \tag{39}$$

where $\triangle t$ is time step integration; subscript n represents $t=n\triangle t$; subscript $(n+1)$ represents $t=(n+1)\triangle t$; β、γ is independent parameters of the control method characteristics. Two integral parameters φ、ϕ are introduced here. A class of new display integral formats is constructed symmetrically

$$\begin{cases}\{X\}_{n+1}=\{X\}_n+\{\dot{X}\}_n\Delta t+(1/2+\phi)\{\ddot{X}\}_n\Delta t^2-\phi\{\ddot{X}\}_{n-1}\Delta t^2\\ \{\dot{X}\}_{n+1}=\{\dot{X}\}_n+(1+\varphi)\{\ddot{X}\}_n\Delta t-\varphi\{\ddot{X}\}_{n-1}\Delta t\end{cases} \tag{40}$$

Suppose the vibration acceleration response of the vehicle system at point $n+1$ is [17]

$$[M]\{\ddot{X}\}_{n+1}+[C]_{n+1}\{\dot{X}\}_{n+1}+[K]_{n+1}\{X\}_{n+1}=\{P\}_{n+1} \tag{41}$$

and $\{\ddot{X}\}_{n+1}=[M]^{-1}\{\tilde{P}\}_{n+1}$. Thus,

ISSN: 2472-3703 DOI: 10.6911/WSRJ.202506_11(6).0005

$$\begin{aligned}\left\{\tilde{P}\right\}_{n+1} &= \{P\}_{n+1} - [K]_{n+1}\{X\}_n - \left([C]_{n+1} + [K]_{n+1}\Delta t\right)\left\{\dot{X}\right\}_n - \\ &\left\{(1+\varphi)[C]_{n+1} + (1/2+\phi)[K]_{n+1}\Delta t\right\}\left\{\ddot{X}\right\}_n \Delta t \\ &+\left(\varphi[C]_{n+1} + \phi[K]_{n+1}\Delta t\right)\left\{\ddot{X}\right\}_{n-1}\Delta t\end{aligned} \tag{42}$$

For the vehicle-equipment coupled system, $[C]_{n+1}$ and $[K]_{n+1}$ in the formulae mentioned above are always the damping matrix $[C]$, stiffness matrix $[K]$ of vehicle system, and $[M]$ is the mas matrix of vehicle. Based on the initial conditions, we obtained

$$\left\{\ddot{X}\right\}_0 = [M]^{-1}\left(\{P\}_0 - [K]\{X\}_0 - [C]\left\{\dot{X}\right\}_0\right) \tag{43}$$

Using recursive integration formulae, the discrete values of displacement, velocity, and acceleration for each step length are calculated stepwise. Notably, as an initial condition, only let $\varphi = \phi = 0$, $\beta = 0.3$, $\gamma = 0.1$, to enable the self-start feature of the integration.

7. NUMERICAL APPLICATIONS

This section concentrates on the result of the numerical simulations regarding the influence of the suspension parameters upon the ride comfort index of vehicle and the vibration severity of the suspended equipment. Such simulations rely on the model and method in the previous sections.

Based on the above parameters, the vibration response of the car body and equipment are calculated for different working conditions by using the numerical method in Section 6. Fig. 7 shows the bounce movement, pitch movement, vertical bending and equipment vertical responses of the vehicle system at the traveling speed of 200 km/h.

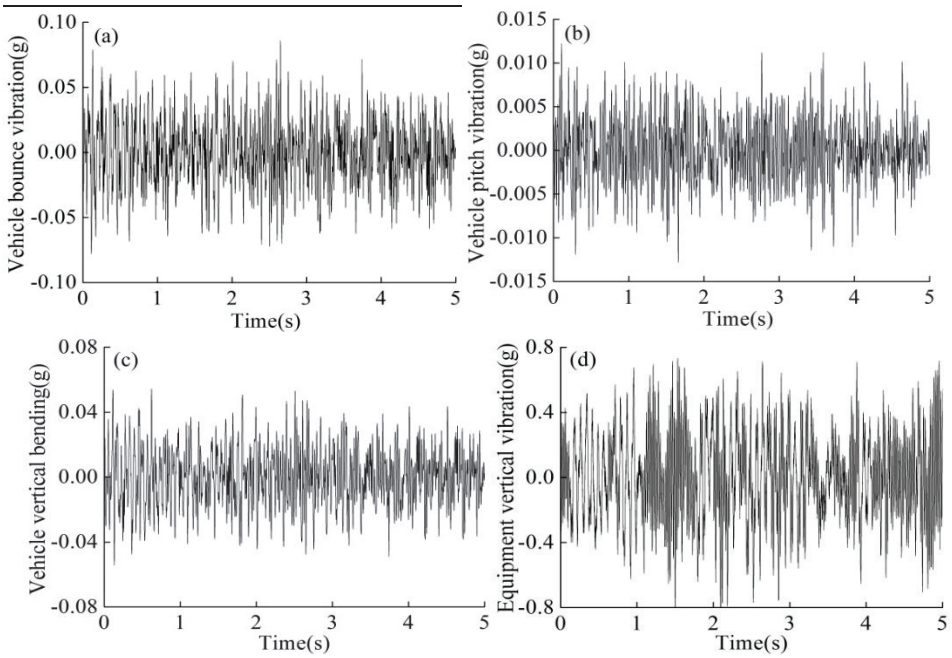


Figure 7. Vibration of vehicle system with speed 200 km/h, (a) Bounce, (b) pitch, (c) Vertical bending in middle car, (d) Equipment vertical bending

With the combination of calculation method of vehicle system vibration index described in section 5 and the obtained vibration history response such as in Fig. 7, we can calculate the ride comfort index and vibration severity. Here, the reference point of the ride comfort index

ISSN: 2472-3703 DOI: 10.6911/WSRJ.202506_11(6).0005

referred to UIC 513R is introduced, and the three critical point: above the front bogie, in the middle of the carbody, above the rear bogie are presented in Fig. 8.

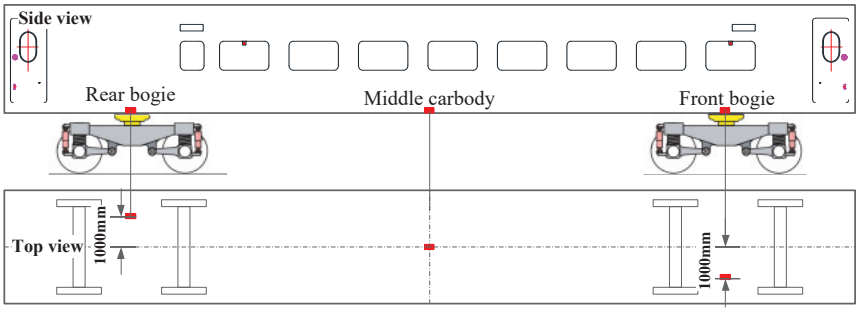


Figure 8. Reference point of the ride comfort index of carbody.

The result of ride comfort index of vehicle and the vibration severity of equipment with different suspension way (elastic or rigid) are exhibited in Figs 9. It can be seen that the ride comfort index of vehicle and vibration severity of equipment increase when the speed is increasing from velocity 100 to 400 km/h. The level of ride comfort index in carbody changes at the three reference points when introduced the elastic suspended equipment in the model of the vehicle. The ride comfort index can be decreased obviously when equipment suspended in elastic way compared to the rigid suspension method. Also the elastic suspension way can enlarge the equipment vibration severity in the same velocity.

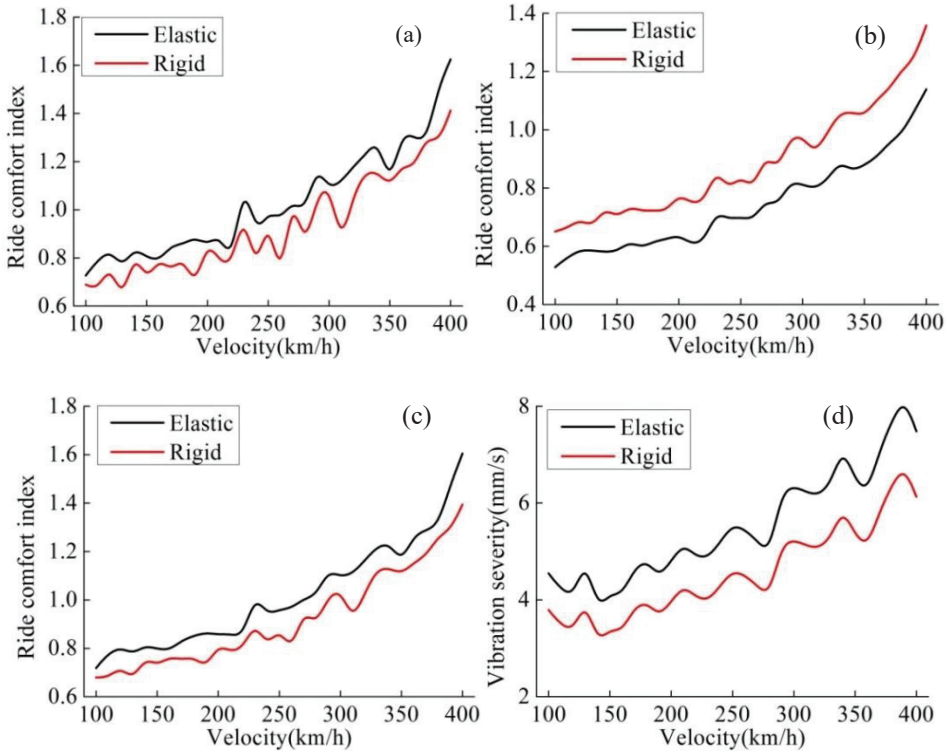


Figure 9. Vibration index of vehicle system with different speed: (a) Above front bogie, (b) In the middle car, (c) Above rear bogie, (d) Vibration severity of transformer.

Figure 10 and Figure 11 represent the distribution of the ride comfort index of three reference point and vibration severity of transformer when the vehicle travels from speed 100 to 400 km/h with track irregularity spectra of German railways as well as the equipment excited. The distribution of the ride comfort index is noticed to be symmetrical with respect to the

ISSN: 2472-3703 DOI: 10.6911/WSRJ.202506_11(6).0005

middle carbody, with different laws in dependence on velocity. In general, the ride comfort index increases along with velocity, but this amplification is not uniform, especially in the middle of the carbody. As a rule, the ride comfort index is lower in the middle than the ends and both of the middle and the end of the vehicle have the same trend. Also the vibration severity of the transformer increases along with the speeds.

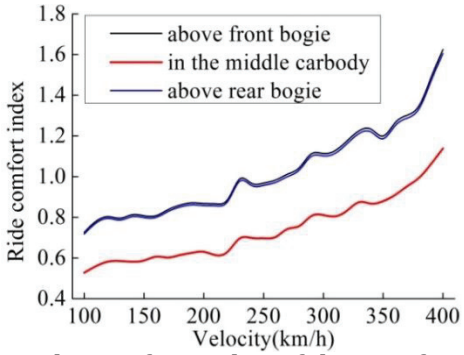


Figure 10. Ride comfort index of three reference point.

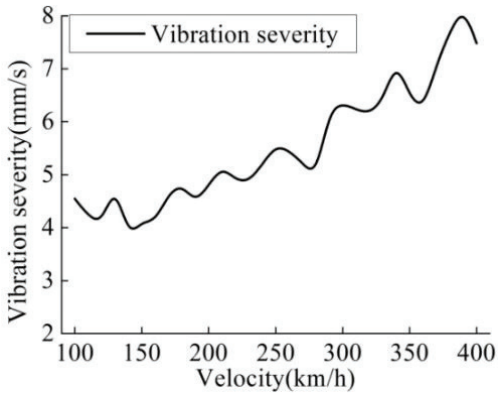


Figure 11. Vibration severity of transformer.

The suspension position, refer to placement of the suspension equipment in rail vehicle, is one of the transformer's main parameters. In figure 3, the suspension is placed in the vehicle mass central point in x axis, so the suspension position is 12.5m. If we place the suspension equipment in the left of mass central point, we mark the position as a small value. By using the numerical method in Section 6, we can get the vehicle vibration results showed in Fig.14 to Fig.17.

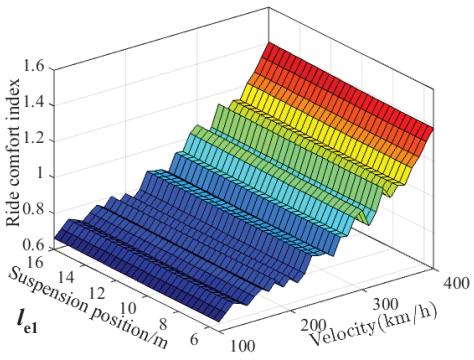


Figure 14. The ride comfort index above front bogie.

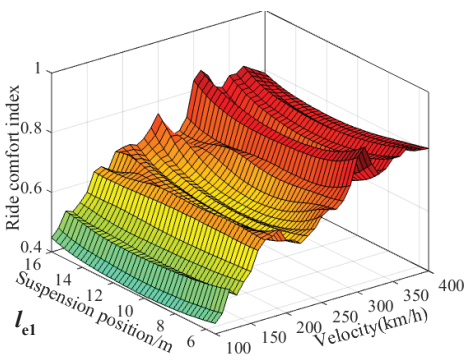


Figure 15. The ride comfor t index in middle carbody.

ISSN: 2472-3703 DOI: 10.6911/WSRJ.202506_11(6).0005

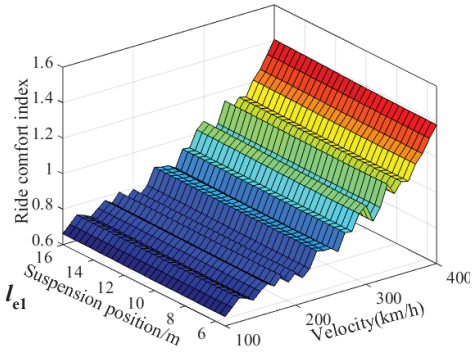


Figure 16. The ride comfort index above rear bogie.

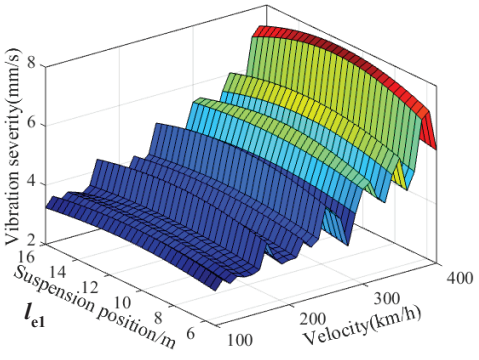


Figure 17. The vibration severity of equipment.

Fig.14 and Fig.16 show the above front and rear bogie ride comfort index respectively in different suspension position and different vehicle speeds. The comfort index increases when the speed is increasing in the same suspension position. The comfort index is less influenced by the suspension position in the same velocity. Fig.15 shows the middle carbody ride comfort index in different suspension position and different vehicle speeds. The comfort index increases when the speed is increasing in the same suspension position. When the vehicle speed is 200 km/h to 300 km/h, the ride index decreases first and then rises as the suspension position increases from 6 m to 16m. Fig.17 shows the vibration severity of equipment in different suspension position and different vehicle speeds. The vibration severity increases when the speed is increasing in the same suspension position. The vibration severity increases first and then decreases as the suspension position increases from 6 m to 16m.

From Fig.14 to Fig.17, it can be seen that the suspension position has a big impact on the middle carbody ride comfort index and on the vibration severity of equipment. While its suspension position has little impact on the above front and rear bogie ride comfort index, also the same as the vibration severity. The closer the suspended equipment to the middle carbody, the more obvious the ride comfort improvement of the middle vehicle will be, also the vibration severity of the equipment is easier to amplify. It looks like that equipment hanging in the middle vehicle is more suitable than other position, so the next study will only consider this condition.

The suspension frequency $\boldsymbol{f_1}$, refer to stiffness of the suspension equipment in rail vehicle, is another one of the transformer's main parameters. In order to facilitate the analysis, the suspension frequency is introduced

$$f_1 = \frac{1}{2\pi}\sqrt{\frac{2\left(k_{e1}+k_{e2}\right)}{m_e}} \tag{44}$$

If the suspension frequency f_1 is high, this means high suspension stiffness of equipment. Obviously, changes in the suspension frequency of the traction transformer have a direct bearing on the ride comfort index and vibration severity. The values of the comfort index and vibration severity are calculated under different speed and suspension frequencies of the equipment (results shown in Figs. 18–21).

ISSN: 2472-3703 DOI: 10.6911/WSRJ.202506_11(6).0005

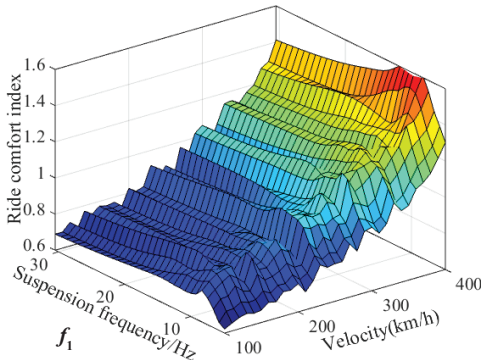


Figure 18. The ride comfort index above front bogie.

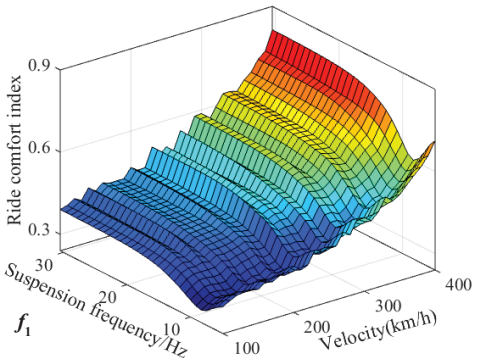


Figure 19. The ride comfort index in middle carbody.

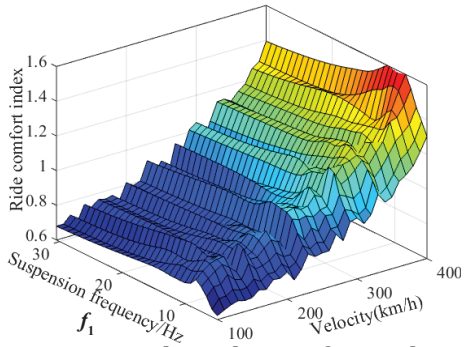


Figure 20. The ride comfort index above rear bogie.

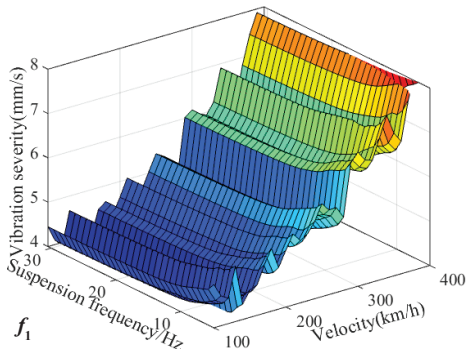


Figure 21. The vibration severity of equipment.

Fig.18 and 20 exhibit the changes in the ride comfort index directly above the bogies. Precisely, the comfort index increases as the traveling speed increases. For each speed class, there exists a peak ride comfort value, the position of which varies almost with the same suspension frequency range:7.4～9.2Hz. The suspension frequency of the traction transformer higher than 9.2Hz can prevent the peak ride comfort index directly above the bogies.

Fig.19 shows the comfort index changes in the middle of the vehicle. The comfort index in the middle of the vehicle first decreases, then increases again with the increasing suspension frequency of the equipment. The comfort index in the middle vehicle has the valley value when the suspension frequency of equipment is 8.5Hz, and the ride comfort index of the middle vehicle do not increase as the suspension frequency increases when f_1 is higher than 16.8Hz.

Fig.21 shows the changes in the vibration severity of the traction transformer; as the traveling speed increases, the vibration severity of the traction transformer increases gradually. Also the equipment vibration severity decreases with the increasing suspension frequency. That is higher suspension frequency of equipment can reduce the transformer vibration severity.

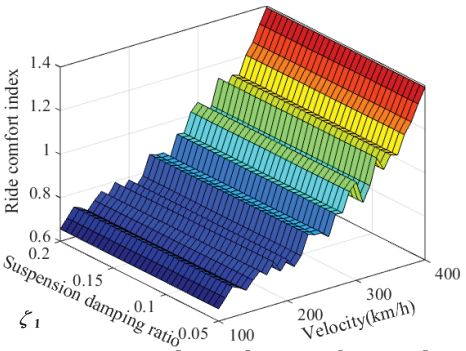


Figure 22. The ride comfort index above front bogie.

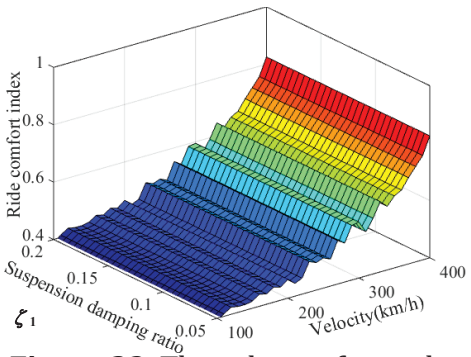


Figure 23. The ride comfort index in middle carbody.

ISSN: 2472-3703 DOI: 10.6911/WSRJ.202506_11(6).0005

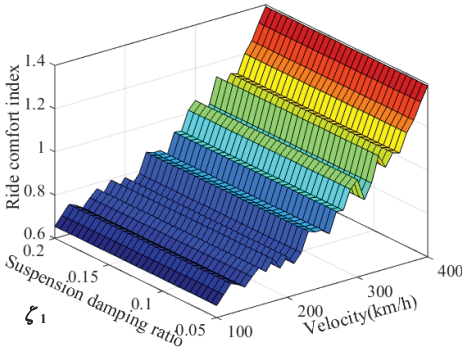


Figure 24. The ride comfort index above rear bogie.

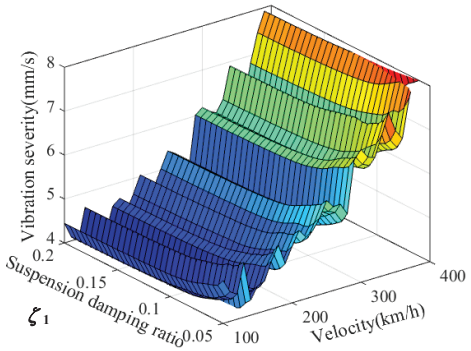


Figure 25. The vibration severity of equipment.

Suspension damping ratio ζ_1 is the third transformer's main parameters. Based on the transformer's suspension parameters, the ζ_1 is given by the following equation

$$\zeta_1 = \frac{2(c_{e1} + c_{e2})}{2\sqrt{2(k_{e1} + k_{e2})m_e}} \tag{45}$$

Fig.22 to Fig.25 shows the results in different suspension damping ratio by using the numerical method in Section 6. Fig.22-24 show the ride comfort index above front bogie, in middle carbody and above rear bogie respectively. It can be seen that the suspension ratio has less impact on the ride comfort index. Fig.25 shows the vibration severity of equipment in different damping ratio and vehicle velocity. The vibration severity decreases as the suspension damping ratio increases in the same vehicle velocity. The suspension damping ratio only affects the vibration severity of the transformer itself.

8. CONCLUSIONS

The suspending of the equipment onto the chassis of high speed train can impact the behaviour of the vertical vibration of the vehicle on account of equipment's large masses. This paper studies this issue based on the vibration index of the vehicle in its three reference points and the vibration severity of equipment. Within the results derived from the numerical simulations, the research lies on the equipment influence, manner of suspension (rigid or elastic) and its suspension parameters, considering the ride comfort index of reference points and vibration severity of equipment.

It has been shown that ride comfort index can be decreased obviously when equipment suspended in elastic way compared to the rigid suspension method. Also the elastic suspension way can enlarge the equipment vibration severity in the same velocity. As a rule, the ride comfort index is lower in the middle than the ends and both of the middle and the end of the vehicle have the same trend.

It is essential to take into account the track irregularity excitation and equipment excitation itself so as to help with examining the dynamic condition in which the suspended equipment can influence the vibration behavior of high speed train.

In terms of the impact of the suspension parameters of the elastically suspended equipment such as suspension frequency f_1, suspension damping ratio ζ_1 and suspension position l_{e1}. The results show that suspension position has little impact on the above front and rear bogie ride comfort index, however it can improve the ride comfort index of the middle vehicle; The ride comfort index above the bogies get the peak values when f_1 is between 7.4~9.2Hz, and the comfort index do not change any more when f_1 is higher than 9.2Hz. The comfort index in the

ISSN: 2472-3703 DOI: 10.6911/WSRJ.202506_11(6).0005

middle vehicle has the valley value when the suspension frequency of equipment is 8.5Hz, and the ride comfort index do not increase as the suspension frequency increases when f_1 is higher than 16.8Hz, also higher suspension frequency of equipment can reduce the transformer vibration severity; Ultimately, the suspension damping ratio only affects the vibration severity of the transformer itself.

REFERENCES

[1] I. Y. Choi et al., The influence of track irregularities on the running behavior of high-speed trains, Proceedings of Institution of Mechanical Engineers Part F Journal of Rail & Rapid Transit, 227 (1) (2013) 94-102.

[2] Yao, Yuan, et al. "Suspension parameters optimum of high-speed train bogie for hunting stability robustness." International Journal of Rail Transportation 8.3 (2020): 195-214.

[3] Huailong S ,Jing Z ,Sheng Q .Linear stability analysis of a high-speed rail vehicle concerning suspension parameters variation and active control [J]. Vehicle System Dynamics, 2023, 61(11): 2976-2998..

[4] Zhongcheng Q ,Shichang H ,Jing N , et al.Vertical Suspension Optimization for a High-Speed Train with PSO Intelligent Method[J].Computational Intelligence and Neuroscience,2021,20211526792-1526792.

[5] Chen, X., Yao, Y., Shen, L., & Zhang, X. (2021). Multi-objective optimization of high-speed train suspension parameters for improving hunting stability. International Journal of Rail Transportation, 10(2), 159–176. https://doi.org/10.1080/23248378.2021.1904444.

[6] Zhu Hai-yan, Li Jie, Yin Bi-chao, et al. Influence of suspension parameters of traction motor on vibration characteristics of traction drive components of high-speed train[J]. Journal of Traffic and Transportation Engineering, 2023, 23(1): 156-169.

[7] Jinying G ,Huailong S ,Fansong L , et al.Field Measurements of Vibration on the Car Body-Suspended Equipment for High-Speed Rail Vehicles[J].Shock and Vibration,2020,2020.

[8] Dumitriu, Mădălina. "Numerical study of the in uence of suspended equipment on ride comfort in high-speed railway vehicles." Scientia Iranica 27.4 (2020): 1897-1915..

[9] Yao, Yuan, et al. "Suspension parameters design for robust and adaptive lateral stability of high-speed train." Vehicle System Dynamics 61.4 (2023): 943-967..

[10] M. Dumitriu, Influence of the vertical suspension on the vibration behavior in the railway vehicles, Nihon Geka Hokan Archiv Für Japanische Chirurgie, 42 (3) (2011) 133–135.

[11] J. Sun, Q. Yang, and Y. Chen, Application of microcomputer in vibration control of internal combustion engine, Mechanical & Electrical Engineering Magazine, 18 (1) (2001) 21–23.

[12] W. M. Zhai, Vehicle-Track Coupling Dynamics, Beijing, Science Press, 2015.

[13] UIC 513R: Guidelines for Evaluating Passenger Comfort in Relation to Vibration in Railway Vehicles, International Union of Railways, 1994.

[14] X. H. Fan, Research on vibration severity for machine condition monitoring, Journal of Academy of Armored Force Engineering, 22 (4) (2008) 46-49.

[15] Y. Sun et al, Modal matching analysis and vibration characteristics of two-stage vibration isolation system, Journal of Vibration Measurement & Diagnosis, 34 (4) (2014) 727-731.